ISSN1027-5495. Functional Materials, 31, No.4 (2024), p. 561-573
doi:http://dx.doi.org/10.15407/fm31.04.561

A novel method for domains simulation in a monolipid membrane

R.Ye. Brodskii[1], O.V. Vashchenko[2]

[1]Institute for Single Crystals, National Academy of Science of Ukraine, 60 Nauky Ave, 61072 Kharkiv, Ukraine
[2]Institute for Scintillation Materials, National Academy of Science of Ukraine, 60 Nauky Ave, 61072 Kharkiv, Ukraine

Received September 3, 2024

Some experiments with biological membranes have shown that a number of dopants can induce spontaneous lateral lipid separation into domains with different physical properties even in a monolipid membrane. Since most such dopants are approved drug substances, one can suppose this phenomenon is relevant to their therapeutic action. Such effect was observed for the dopants with bimodal adsorption. We assumed that the underlying mechanism of such dopant-induced domain formation is preferential dopant binding 'like the surroundings' rather than 'unlike the surroundings'. In the present work, the simulation method based on the mechanism of preferential dopant binding to monolipid membrane has been developed. The domains sizes were calculated using a simple procedure similar to that used for percolation clusters. Using the method, the mean size of the largest lipid domains was shown to grow by orders of magnitude under moderate increase in the extent of preferential dopant binding. This finding affirms preferential binding as a governing mechanism of lipid domain formation in the systems explored. Adsorption isotherms for the case of bimodal sorption, albeit irrespective of surrounding, were analytically obtained. They coincide with the corresponding numerical simulation results. The method can be easily modified for exploring any systems with polymodal binding to a network of connected sites, so it may see increased application in the future for various physical, chemical, biological, biophysical and other systems.

Keywords: model lipid membranes, lipid domains, bimodal adsorption, simulation, self-structuring, percolation clusters.

Новий метод моделювання доменів у моноліпідній мембрані. *Р.Є. Бродський, О.В. Ващенко*

Експерименти з біологічними мембранами показали, що деякі домішки можуть індукувати спонтанне латеральне розділення ліпідів на домени з різними фізичними властивостями навіть у моноліпідних мембранах. Оскільки більшість таких домішок є схваленими лікарськими речовинами, то вказане явище може певною мірою стосуватися їх терапевтичної дії. Ми припустили, що механізмом, який лежить в основі такого індукованого домішкою утворення доменів, є переважне зв'язування домішки 'подібно до оточення' у порівнянні з 'протилежно до оточення'. У даній роботі розроблений метод чисельного моделювання, який базується на механізмі переважного зв'язування домішки у моноліпідній мембрані. Розміри доменів були обчислені з використанням процедури, аналогічної тій, що застосовується для перколяційних кластерів. З використанням вказаного методу, було показано, що середній розмір найкрупніших ліпідних доменів зростає на порядки з невеликим збільшенням ступеню переважного зв'язування домішки. Це підтверджує, що механізм переважного зв'язування є одним з ключових для утворення ліпідних доменів в досліджуваних системах. Аналітично було отримано ізотерми бімодальної адсорбції для випадку її незалежності від оточення. Вони співпадають з відповідними результатами чисельного моделювання. Метод легко модифікується для будь-яких систем, де наявне полімодальне прикріплення на зв'язаних один з одним сайтах, тож в майбутньому він може набути більш широкого застосування для дослідження різноманітних фізичних, хімічних, біологічних, біофізичних та інших систем.

List of symbols

E_h, E_l	the binding energies of dopant sorption by h-type or l-type
h, l	two dopant binding types (modes), on the membrane surface (h) or in its interior (l)
n_i $i = 0, h, l$	* the number of the nearest neighbor cells of i-type around a given binding cell
p_f	* the probability of a dopant presence in the vicinity of a binding cell during the time corresponding to a given simulation step
p_h, p_l	the probability that a dopant molecule adsorbs to a binding site by h-type or l-type, correspondingly
$\tilde{p}_h, \tilde{p}_l$	have the same sense as p_h, p_l yet disregarding another binding mode
p_{h-}, p_{l-}	the probability of a dopant molecule to desorb from a binding site during a given simulation step
p_{ij} $i = 0, h, l$, $j = h, l$	* the probability of a dopant molecule to adsorb to a binding site by j type if all the nearest neighbor cells contain dopants bound by i type (0 indicates an 'empty' binding site)
$\tilde{p}_{ij}$ $i = 0, h, l$, $j = h, l$	has the same sense as p_{ij} yet disregarding another binding mode
p_{other}	the common designation for p_{lh}, p_{hl}
p_{same}	the common designation for p_{hh}, p_{ll}
S	the total amount of simulated cells
S_h, S_l, S_0	numbers of the cells with h-type and l-type dopant binding or without dopant
W, H	* dimensions (width and height, in numbers of binding sites) of a simulated membrane lattice.

* parameters of the simulation

1. Introduction

Lipid membrane is a self-structuring medium which can be efficiently considered as a quasi-two-dimensional nanostructure, particularly in regard to sorption and diffusion processes [1–3]. Such media are spontaneously formed by amphiphilic lipid molecules in water subphase, both *in vivo* and *in vitro*. Polar lipid moieties ('heads') form membrane surface and non-polar ones ('tails') form membrane interior (Fig. 1). Among a variety of intriguing features of lipid membrane medium, there is its ability for lipid domains formation, i.e. for lateral lipid separation into regions with different properties. Such separation either originates from limited miscibility of membrane constituents (different lipid species) or is induced by various guest substances (dopants). These two reasons often occurs simultaneously, e.g. on forming complex lipid-protein aggregates called lipid rafts [4–6].

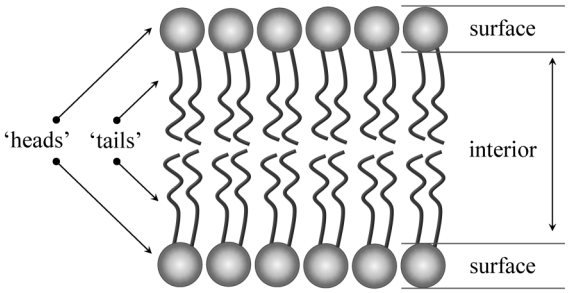

Fig. 1. A scheme of lipid membrane structure. Lipid 'heads' and 'tails' form, correspondingly, membrane polar surface and non-polar interior.

However, dopant-controlled lipid domain formation takes place even in a monolipid membrane, i.e. in a membrane comprised of lipids of the same species. To our knowledge, this is a particular and understudied kind of lipid domains. It was experimentally shown that a monolipid membrane can be separated into dopant-enriched and dopant-depleted lipid domains, e.g. in the presence of such drugs as an anticoagulant coumarin [7] and an antibiotic surfactin [8]. Whilst there are some examples of occurrence of two different types of dopant-enriched domains, as it was observed in the presence of an antibiotic gramicidin S [9,10] and *L*-tryptophane [3], an essential amino acid with sedative properties. Since all the above-mentioned domain-inducing dopants are pharmacologically active substances, the phenomenon might be strictly related to their medico-biological relevance.

Both gramicidin S and *L*-tryptophane are reported to exhibit bimodal adsorption, i.e. there are two modes of membrane binding, namely, polar surface sorption or non-polar interior embedding [11,12]. They form two types of lipid domains with specific thermodynamical characteristics, different from neat membrane. This phenomenon was evidenced by differential scanning calorimetry (DSC) technique *via* observation of different membrane melting peaks, none of them match the neat membrane. So, one can suppose that the membrane portions with different transition temperature are those with dopants absorbed either on the membrane surface or in its interior.

However, existence of different binding modes *per se* seems quite insufficient to emerge lipid domains since a dopant may bind in both types homogenously throughout the membrane. So, the main idea implicit in the suggested model is as follows: lipid domains formation occurs due to the fact that dopant binding 'like the surroundings' is energetically favorable, whereas its binding 'unlike the surroundings' is energetically unfavorable. In other words, dopant molecules prefer the binding type which is already implemented in the surroundings of a given binding site. Hence, the probability of dopant binding in a certain type elevates if the surroundings contains dopant molecules bound in the same mode and, correspondingly, reduces if the surroundings contains the molecules bound in another way.

The phenomenon of lateral lipid separation and lipid domains formation has been investigated in diverse aspects, namely, in experimental and theoretical studies, as well as computer simulations. An extensive review of the appropriate experimental methods is given in the work [13]. In the scope of the present work, let us emphasize on theoretical and simulation approaches used in this field.

The closest to the above experimental findings is the work [14], where ion-induced lipid domains formation is studied in a composite (not monolipid) membrane containing acidic due to decreasing of the Debye screening length. In another closely related work [15], lateral lipid separation caused by adsorption of basic peptides was investigated in a similar membrane. Besides, a number of works quantitatively examines composite lipid membranes by means of related simulation method [16–18]. In these works, a lipid membrane is considered as a set of unit objects ('points' of a pattern) arranged in the hexagonal lattice, whereas the lipid phase separation is not dopant-induced. Such a level of abstraction allows simulation of a large number of lipids over long timescales.

Variety of numerical simulation approaches is described in the reviews [19,20]. Most of works are devoted to lipid phase separation study by means of the coarse-grained simulation basis [21–23]. Such approach allows long timescale simulation of rather large lipid lattices, though their dimensions are typically much less than those used in the present study. Detailed molecular simulation is less commonly used for such purposes since it further restricts both the timescale and the lattice dimensions. Atom-scale molecular dynamics simulations is applicated to investigation of nanoscaled lipid domains, as well as to large-scale properties of raft-like membrane environments *via* obtaining lateral pressure profiles [24]. Some thermodynamic parameters can be obtained from simulation data [25].

The analytical approaches are typically based on the Ginzburg-Landau theory, i.e. on representation of the free energy as a function of the order parameter. On the basis of such a model, the phase diagrams are obtained [26], with different regions corresponding to a neat membrane as well as various kinds of lateral lipid separation [26–28]. A good agreement between the analytical and the coarse-grained simulation results is reported [29]. Domains appearance is also shown on the basis of dependence of the free energy on cholesterol molar fraction, from the condition of instability of homogenous state [30] as well as on the bases of phase diagrams. The domains size is estimated from the minimization of the free energy [31] as well as from the Fourier decomposition of the free energy [32]. Membrane deformation (the changes in curvature) resulted from the lateral lipid separations is also examined analytically [33]. Some authors use mean-field theory, however, they suggest the expressions of free energy based on general thermodynamics [34–36] instead of the Ginzburg-Landau theory. Diffusion processes in percolation system formed by lipid domains and other related problems are also theoretically studied [37].

Thus, in all the cases reported, a composite (not monolipid) membrane was chosen as the object of study. Besides, relations between lipid domains formation and dopant sorption from surrounding media were not examined. To the best of our knowledge, lipid domain formation caused by two-mode dopant adsorption is firstly explored theoretically in the present work.

For this purpose, a method of lipid domains simulation in a monolipid membrane has been developed. It consists in simulation of random adsorption/desorption of small dopant molecules in two different ways in a hexagonal lattice of lipid molecules. Domain is determined as a set of binding cells filled in the same way, such that one can pass between any cells along a chain of the nearest neighbor (NN) cells. The process is simulated prior to steady state, then domain sizes are determined.

The main distinguishes of the method suggested from those used in literature are:

(i) simulation of two mutually incompatible dopant binding modes;
(ii) dependence of dopant binding probability on surroundings of a binding site;
(iii) just binding (or non-binding) and unbinding events depending on surroundings are taken into account, without extensive physical detalization, which allows one to simulate large steady lipid domains;
(iv) possibility to simulate and explore relatively large membrane areas (up to $\sim 10^5 - 10^6$ lipids, i.e. up to $\sim 0.1 - 1$ μm of membrane surface) during the times enough to obtain a steady pattern of large lipid domains by means of an ordinary personal computer.

Thus, the aim and the result of the developed simulation method are obtaining and analysis of large steady lipid domains arising in a monolipid membrane as a result of two-mode dopant binding.

2. Simulation method

As it was mentioned above (see Sec. 1), two dopant binding modes are considered, namely, to membrane surface or membrane interior. Then we will refer to the former one as h-type ('high', or 'heads' of lipids which form membrane surface) and to the latter one as l-type ('low'). We also will refer to binding cells containing dopants as h-type or l-type cells. A lipid membrane was simulated as a lattice of $N = W \times H$ cells each of them can be in three states, 'empty', 'h-type', 'l-type'.

Let us describe in more details the simulated lipid lattice, the simulation protocol, as well as the rules for determining the NN (actually, the 1st coordination shell) and sorption/desorption probabilities depending on the surroundings.

2.1 Selecting a binding lattice type and the rules for determining the nearest neighbors

In some approximation, a lipid membrane could be considered as a hexagonal lipid lattice [38], as it is visualized in Fig. 2, a. If dopant molecules bind near lipid molecules then binding sites will form the same lattice type. Then NN of such binding sites lattice will comprise 6 cells, as it shown in Fig. 2, a with arrows. A unit cell of such a lattice can be chosen in several ways. The most obvious one is a hexagon, as it is shown in Fig. 2, a. Another way is a rhombus cell (Fig. 2, b) with vertices in the centers of 4 neighboring lipid molecules (we will return to this just below). Such a unit cell comprises a lipid molecule, as it should be, as well as a binding site near it.

However, in the general case, it seems reasonable to consider dopant binding equidistantly from neighboring lipid molecules. Such binding sites lattice is shown Fig. 2, b with triangles. The upward-pointing triangles sign the binding cells with a lipid molecule on the top (navigating by Fig. 2, b); the downward-pointing triangles sign the cells with a lipid molecule at the bottom. There is no distinguish between physical properties of these two cell types for the current study. However, some distinguishes can arise in a field parallel to the membrane surface which causes certain shifts of dopant molecules. For example, if such a filed is directed upward (navigating by Fig. 2, b) then dopant particles will move closer to lipid molecules in the first type cells and, correspondingly, move from lipid molecules in the second type cell. So, dopant binding to some type cell could become preferable. For the first type, there are NN cells left, right and bottom, whereas for the second type, they are left, right and top. As one can see, such binding sites are arranged in horizontal lines and vertical columns, but with certain shifts. These shifts are insignificant for the present simulation since distance from a cell to all their NN remains the same. Thus, it is very convenient to simulate the lattice in a rectangular array which is common for computer programs.

The binding lattice is hexagonal, same as the lipid lattice in Fig. 2. Its unit cell can be chosen as hexagon, but a rhombus cell (see Fig. 2, b) seems more naturally, because it explicitly encompasses two different binding sites (one of each type, as it should be) and a lipid molecule.

In terms of graph theory or percolation theory binding lattice of "near lipids" type (Fig. 2, a) is called a "triangular lattice" because if one connects the centers of the cells with lines, the lattice will look like a set of triangles (with the tips up down). We will not use this term for the simulated lattice to avoid confusion with the crystal lattice of lipids. The binding lattice of the "equidistant from lipids" type (Fig. 2, b) is called a "honeycomb lattice" in graph theory for similar reasons. Such a lattice is by definition "dual" to the "triangular lattice". In particular, this means that in conventional percolation problems, when a node can only be in two states – conducting or not – the percolation threshold values for the above two lattices sum to one.

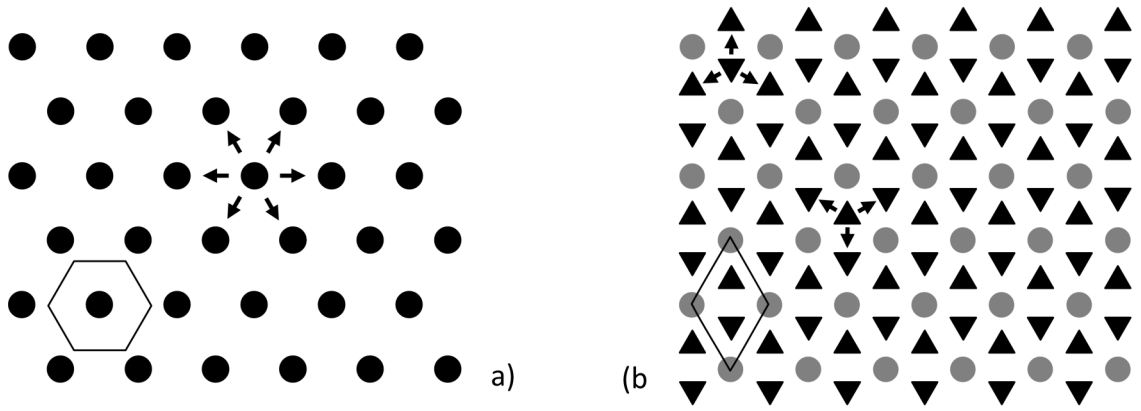

Fig. 2. Binding sites lattices for simulation: in the case of dopant binging near a lipid molecule (a) or equidistantly from neighbouring lipid molecules (b). Dopant binding sites are marked in black circles or triangles; grey circles sign location of lipid molecules. Unit cells are shown with lines. Arrows point to the nearest neighbour cells.

For illustration of method application, we use in this work the lattice shown in Fig. 2, b. In order to avoid boundary effects (which can be significant due to dependence of binding probability on surroundings) we used cyclic boundary conditions. In all the simulation experiments, $W = H$ was in the order of several hundred. In the resulting simulation patterns (see Sec. 4), a point corresponds to a binding cell. These points are arranged in a regular rectangular array. But, as it was mentioned above, binding cells do not arrange in a such regular lattice, so the patterns become slightly distorted. However, the dimension of this distortion is of the order of a point size, so it seems insufficient for large-scaled structures. Meanwhile, the pattern presentation 'a point is a cell' allows us to display much more cells than in Fig. 2, where a cell is displayed by a group of points.

2.2. Simulation procedure

An elementary simulation step was as follows. A cell was randomly chosen from $N = W \times H$ array. If the cell was in 'empty' state, then the presence of a dopant molecule in its vicinity was primarily determined (i.e. physically – during the time corresponding to a simulation step). Corresponding probability p_f was pre-set as a simulation parameter. Physically, p_f reflects dopant concentration in the system.

In the case of absence of a dopant molecule, the next simulation step was started. Otherwise, the probabilities of three different events were used, namely, dopant adsorption on the membrane surface (p_h), adsorption in the membrane interior (p_l) and no adsorption (p_0). The sum of these probabilities is equal to one. These probabilities were calculated accounting for the cell surroundings by the procedure described in Sec. 2.3. It was randomly determined which of these events occurred. If an adsorption event took place, a cell changes its state from 'empty' to 'h-type' or 'l-type'; otherwise the cell state remains unchanged. If a cell already contained an adsorbed dopant molecule, the desorption probabilities p_{h-} or p_{l-} were used, which are also obtained preliminary for h-type and l-type cells, correspondingly (see Sec. 2.3). It was randomly determined if a desorption event occurs. If so, a cell becomes 'empty', otherwise, the cell state remains unchanged.

There was the following procedure for determining of a random event occurrence. A random number was generated in the interval $[0,1]$ and compared to the corresponding probability value. If the number was less than or equal to the probability value, an event was deemed to have occurred; if it was higher, an event was deemed to have not occurred. To determine if one of mutually incompatible events occurs, such as adsorption on the membrane surface or in the interior, this random number was compared to the probability p_1 of one of the events, as it is described above. If this event has occurred, the comparison is finished. Otherwise, it is checked if the generated number match to the interval $(p_1 , p_1 + p_2]$ to determine if another event has been occurred. The condition $p_1 + p_2 \le 1$ is checked (or is guaranteed by the calculation procedure). If the generated number is higher than $p_1 + p_2$ then no of the events have occurred.

A simulation generation is defined as $N = W \times H$ of elementary simulation steps. In this sense, a generation is an analog of a full crawl of all the simulated cells, however,

with random cell choosing instead of sequential, which closer mimics adsorption/desorption processes. The amount of the generations was chosen to be sufficient for obtaining a dynamically steady pattern (see Sec. 4). Typical number of generations used in this work was about several thousands.

2.3. Determining of absorption/desorption probabilities

The probabilities for each binding mode, h or l, were pre-set for the cases of homogenous surroundings ('empty cells only', 'h-type cells only', 'l-type cells only'). They are p_{0h}, p_{hh}, p_{lh}, p_{0l}, p_{hl}, p_{ll}, where the first subscript index indicates the type of homogeneous surrounding and the second one specifies the type of binding. In total, we pre-set six such parameters as well as the probability p_f introduced in Sec. 2.2. We met the condition $p_{ih} + p_{il} \le 1$ ($i = 0,h,l$) because l-type and h-type binding are two mutually incompatible events, and the third one is the absence of binding (with probability $1-(p_{ih} + p_{il})$).

Note that the sums $p_{hi} + p_{li}$, with the same second subscript index, do not have a clear physical sense of a certain event probability. Albeit these are convenitent characteristics of binding by a certain type ($i = h,l$) in general, anywhere in the system. If we additionally assume $p_{0i} = \frac{p_{hi} + p_{li}}{2}$, then $\frac{1}{3}\cdot p_{0i} + \frac{1}{3}\cdot p_{hi} + \frac{1}{3}\cdot p_{li} = \frac{p_{hi} + p_{li}}{2}$, i.e. $\frac{p_{hi} + p_{li}}{2}$ will be equal to the probability of dopant binding to a cell surrounded by equal number of cells of each type.

The simplest way to determine the binding probability for combined surroundings is the arithmetic average by NN cells. For example, h-type binding probability is $p_h = \frac{1}{n}\sum_{k=1}^{n} p_{\{k\}h}$ where n is the number of cells in NN (e.g. 6 or 3, as it is depicted in Fig. 2). Symbol $\{k\}$ denotes the k$^{\text{th}}$ cell state, i.e. $\{k\} = 0,h,l$. The expression for p_l is similar, whereas $p_0 = 1-\left(p_h + p_l\right)$. In this way of calculation, the probability of each binding type obviously grows as the number of the same type cells increases (if $p_{hh} > p_{lh}$, $p_{ll} > p_{hl}$) and diminishes as the number of the another type cells increases. The corresponding desorption probability is $p_{i-} = 1 - p_i$, $i = h,l$.

The main disadvantage of such a way of probabilities determination is lack of physical basis, since there are no physical reasons for binding probability to be the arithmetic average. So, the way for probabilities determination through binding energies has been developed (see the next section), which seems more physically reasonable.

Determining of absorption/desorption probabilities using binding energy

For the sake of clarity, let us first consider the case of a single binding mode. We assume that a binding event occurs when the kinetic energy of a dopant molecule in the moment of binding is less than a certain threshold value E, which we will call binding energy. Let us also assume that dopant molecules are characterized by exponential distribution of energies. Then the binding probability is $\tilde{p} = 1 - \exp\left(-\frac{E}{kT}\right)$ (tilde marks the values in the case of a single binding mode). Let the binding energy irrespective of the cell surroundings is E_c and NN cells are able to shift it, so that the total shift is equal to the sum of shifts induced by each NN cell. If this cell is 'empty' the shift is ΔE_0, otherwise it is ΔE_+. The shifts can be either positive or negative, i.e. the binding energy (and the corresponding binding probability) can be increased or decreased.

Let the binding probabilities for homogenous NN surroundings are $\tilde{p}_0$ (all 'empty') and $\tilde{p}_+$ (all 'filled', i.e. 'not empty'). Then $\tilde{p}_0 = 1 - \exp\left(-\frac{E_c + n\Delta E_0}{kT}\right)$ and $\tilde{p}_+ = 1 - \exp\left(-\frac{E_c + n\Delta E_+}{kT}\right)$ where n is the number of NN cells. In the general case, there are n_0 'empty' neighbor cells and n_+ 'filled' ones ($n_0 + n_+ = n$), so that $\tilde{p} = 1 - \exp\left(-\frac{E_c + n_0\Delta E_0 + n_+\Delta E_+}{kT}\right)$. Expressing $\Delta E_0, \Delta E_+$ by $\tilde{p}_0, \tilde{p}_+$, we obtain $\Delta E_i = -\frac{E_c + kT\ln\left(1-\tilde{p}_i\right)}{n}$, $i = 0;+$. Then

$$\tilde{p} = 1 - \sqrt[n]{\left(1-\tilde{p}_0\right)^{n_0}\left(1-\tilde{p}_+\right)^{n_+}},$$

or $\tilde{p} = 1 - \sqrt[n]{\prod_{j=1}^{n}\left(1-\tilde{p}_{\{j\}}\right)}$ where the product is taken over all NN cells and $\{j\}$ is the cell status, 0 ('empty') or + ('filled'), or $\tilde{p} = 1 - \mathbf{G}\left(1-\tilde{p}_{\{j\}}\right)$, where $\mathbf{G}(\cdot)$ is the geometric mean over the values for all NN cells.

Moving to two binding modes, several matters are of note:

§1. There are three types of cell state $(0,h,l)$ instead of two $(0,+)$, as well as two binding probabilities, $\tilde{p}_h$ and $\tilde{p}_l$, instead of one, $\tilde{p}$ (see §2). There are six pre-set parameters, $\tilde{p}_{0h}$, $\tilde{p}_{hh}$, $\tilde{p}_{lh}$, $\tilde{p}_{0l}$, $\tilde{p}_{hl}$, $\tilde{p}_{ll}$, instead of two, $\tilde{p}_0$, $\tilde{p}_+$. Then, similar to the above reasoning, the expressions for $\tilde{p}_i$ will be in the form

$$\tilde{p}_i = 1 - \sqrt[n]{\left(1-\tilde{p}_{0i}\right)^{n_0}\left(1-\tilde{p}_{hi}\right)^{n_h}\left(1-\tilde{p}_{li}\right)^{n_l}}, \qquad (1)$$

where $i = h,l$; n_0, n_h, n_l are the number of NN cells in the corresponding state. This expression can be rewritten as $\tilde{p}_i = 1 - \sqrt[n]{\prod_{j=1}^{n}\left(1-\tilde{p}_{\{j\}i}\right)}$, or $\tilde{p}_i = 1 - \mathbf{G}\left(1-\tilde{p}_{\{j\}i}\right)$.

§2. Probabilities $\tilde{p}_h$, $\tilde{p}_l$ differ from p_h, p_l introduced above (Sec. 2.2). Actually, $\tilde{p}_h$, $\tilde{p}_l$ are the probabilities that the kinetic energy of a dopant molecule is less than its binding energy by the corresponding binding type in a given cell. However, if the kinetic energy appeared to be less than the lowest binding energy (i.e. less than the both energy values) then a dopant can bind in either of two modes albeit do bind in only one of them, since these are mutually incompatible events. The values p_h, p_l are just the probabilities of such mutually incompatible events, whilst $\tilde{p}_h$, $\tilde{p}_l$ are the corresponding binding irrespective of another binding mode. The sum $\tilde{p}_h + \tilde{p}_l$ can be larger than one.

In order to obtain p_h, p_l using $\tilde{p}_h, \tilde{p}_l$ expressed by (1), one can reason as follows. If the kinetic energy of a dopant molecule is higher than both binding energies, a dopant will not bind; if the energy is lower than one of them but higher than another, a dopant will bind in the type corresponding to the higher energy; if the energy is lower than the both binding energies, than a dopant will bind in either type with an equal probability. Let us assume, for example, that $E_h < E_l$. Then the probability $\tilde{p}_h$ that the energy of a dopant molecule in the moment of binding is lower than E_h is the probability that it is lower than the both binding energies. In accordance with the above, a dopant can bind to membrane by either of two types, and the probability for h-type binding is $p_h = \frac{1}{2}\tilde{p}_h$.

In this example, the probability of l-type binding encompasses two components, namely, the probability that the dopant energy is lower than E_l but higher than E_h, and a half of the probability that the energy is less than E_h, i.e. $p_l = \left(\tilde{p}_l - \tilde{p}_h\right) + \frac{p_h}{2}$ or $p_l = \tilde{p}_l - \frac{p_h}{2}$.

So, p_h, p_l can be obtained using $\tilde{p}_h$, $\tilde{p}_l$ as:

if $\tilde{p}_h < \tilde{p}_l$ then $p_h = \tilde{p}_h / 2$, $p_l = \tilde{p}_l - \tilde{p}_h / 2$;

otherwise $p_l = \tilde{p}_l / 2$, $p_h = \tilde{p}_h - \tilde{p}_l / 2$.

Note that $p_h + p_l \le 1$ as it should be.

§3. Parameters $\tilde{p}_{0h}$, $\tilde{p}_{hh}$, $\tilde{p}_{lh}$, $\tilde{p}_{0l}$, $\tilde{p}_{hl}$, $\tilde{p}_{ll}$ are not the pre-set parameters p_{ij} described above. They are the binding probabilities without accounting for another binding type, similar to $\tilde{p}_h$, $\tilde{p}_l$ (see §2). In order to obtain these parameters from the pre-set p_{ij} for substitution into (1), we can applicate the procedure described at the end of §2 to each pair p_{ih}, p_{il}, $i = 0,h,l$, but in the inverse way. So, we obtain:

if $p_{ih} < p_{il}$, then $\tilde{p}_{ih} = 2p_{ih}$, $\tilde{p}_{il} = p_{il} + p_{ih}$;

otherwise $\tilde{p}_{il} = 2p_{il}$, $\tilde{p}_{ih} = p_{ih} + p_{il}$.

§4. Probability of dopant desorption is reasonable to be assumed $p_{i-} = 1 - \tilde{p}_i$ $(i = h,l)$ instead of $1 - p_i$ since desorption is determined by its current binding type irrespective of another binding mode.

§5. Choosing pairs p_{ih}, p_{il} such as $p_{ih} + p_{il} = 1$ seems to be convenient for simulation procedure (due to faster domains growth). However, it should not be used for the case of determination of absorption/desorption probabilities using binding energy because in this case some $\tilde{p}_{ij}$ will be equal to one. It is not convenient for calculations because uncertainties of the type 0^0 will appear in (1). They can be solved easily enough, because if cells of a certain type are absent in NN then they do not affect $\tilde{p}$. However, a specific part of the algorithm should be provided for this particular case. Besides, $\tilde{p}_{ij} = 1$, i.e. assured adsorption disregarding another binding type, means the infinite binding energy which seems senseless from physical viewpoint.

3. Determining the domain size

Determining the size of lipid domains is a challenge, both for experimental [39] and simulation approaches, due to complexity of the domain definition. We will use the following simple considerations. As it was mentioned above, a domain was determined as a connected area of the cells of the same type, i.e. binding sites containing dopant molecules bound by the same mode, such that one can reach any site

from another one by moving along a chain of the NN cells.

For simulation, the binding sites lattice was selected with dopant binding equidistantly from neighboring lipid molecules (Fig. 2, b). This lattice type is convenient to be projected onto an ordinary rectangular array since the cells are arranged in rows and columns, though with certain difference in NN (see Sec. 2.1). To simulate another lattice type (Fig. 2, a) in a rectangular array, the lattice cells can be projected onto the array, as shown in Fig. 3. As one can see, NN in the "rectangular" representation is a little different for odd and even rows (see the arrows). In either case, the nearest elements locate left, right, up and down; however, the cells in even rows have the nearest elements in the previous and the next lines with a column number greater by 1, whereas for odd rows they are smaller by 1.

In order to calculate the number of cells in a connected area (domain), the "depth-first search" algorithm was used (non-recursive variant was chosen due to large number of simulated cells). The cells were taken as vertices of a graph, the links to NN cells were considered as its edges. The domains size was determined separately for h-type, l-type and 'empty' cells.

Actually, the domain sizes defined in such a way are the areas of cluster comprising the cells of the same type. Such clusters are very similar to percolation clusters by their structure. Indeed, they are branched and contain inside some inclusions of other type cells, which are not the cluster parts. Apparently, the lipid domains revealed in experiments (see Sec. 1) are only mostly composed of cells of the same type, but contain inside some minor inclusions of other type cells. So, the determined domain sizes are approximate, though the discrepancy should not be sufficient for quite large domains (~ 10^2 cells and more).

4. An example of the method application

In this section, we demonstrate some applications of the method developed. For the sake of clarity, we will use symmetrical values of the probabilities, $p_{hh} = p_{ll}$, $p_{hl} = p_{lh}$, i.e. equal probabilities for a dopant to be adsorbed in similar and distinct NN surroundings. We will denote the first pair of values $p_{hh} = p_{ll} = p_{\text{same}}$ and $p_{hl} = p_{lh} = p_{\text{other}}$. Binding probabilities in the surroundings of 'empty' NN cells can be defined as $p_{0h} = p_{0l} = \dfrac{p_{\text{same}} + p_{\text{other}}}{2} = p_0$. So, the extent of preferential dopant binding can be characterized either by $p_{\text{same}} : p_{\text{other}}$ or $p_{\text{same}} : p_0$ ratios.

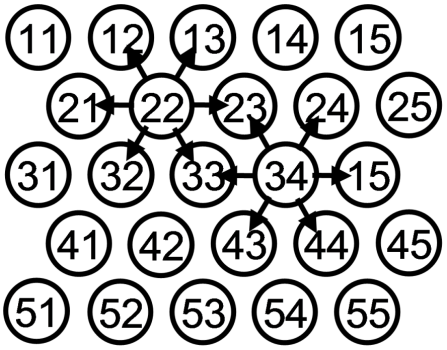

Fig. 3. Matching of the array elements to cells of the binding sites lattice in the case when a dopant is bound to lipid molecules. The circles represent binding sites; the numerals indicate the numbers of the array elements (an array 5×5 is shown). Each number consists of two parts, the row number and the column number. Directions of the links to NN cells are shown with arrows.

Fig. 4 demonstrates some resulting simulation patterns obtained for different $p_{\text{same}} : p_{\text{other}}$ ratios, i.e. for different extent of the preferential binding (certain fragments are represented, so cyclic boundary conditions are not shown). As one can see, the number of 'empty' cells is relatively low since the values were set rather high ($p_{\text{same}} + p_{\text{other}} = 0.99$ and $p_f = 0.95$). Similar patterns were observed experimentally, in particularly, in Langmuir-Blodgett monolayers [40]. Below (Sec. 6), some actual physical parameters corresponding to these probability values are estimated and the obtained values are found to be quite believable.

During the simulation, the systems came to the dynamic equilibrium by about the 500^{th} – 1000^{th} generation depending on $p_{\text{same}} : p_{\text{other}}$. After that, the general number of cells of each type and the characteristic sizes of the corresponding domains remained generally unchanged (all the patterns shown in Fig. 4 correspond to the 5000^{th} generation). With $p_{\text{same}} : p_{\text{other}}$ increased, the domains seem to become larger and less rugged, i.e. more condensed. However, the apparent domain size can differ from the real one, so this observation should be confirmed by calculations. The following confirms that the mean size of the largest domains increase with $p_{\text{same}} : p_{\text{other}}$ though some small inclusions remain for whatever large $p_{\text{same}} : p_{\text{other}}$.

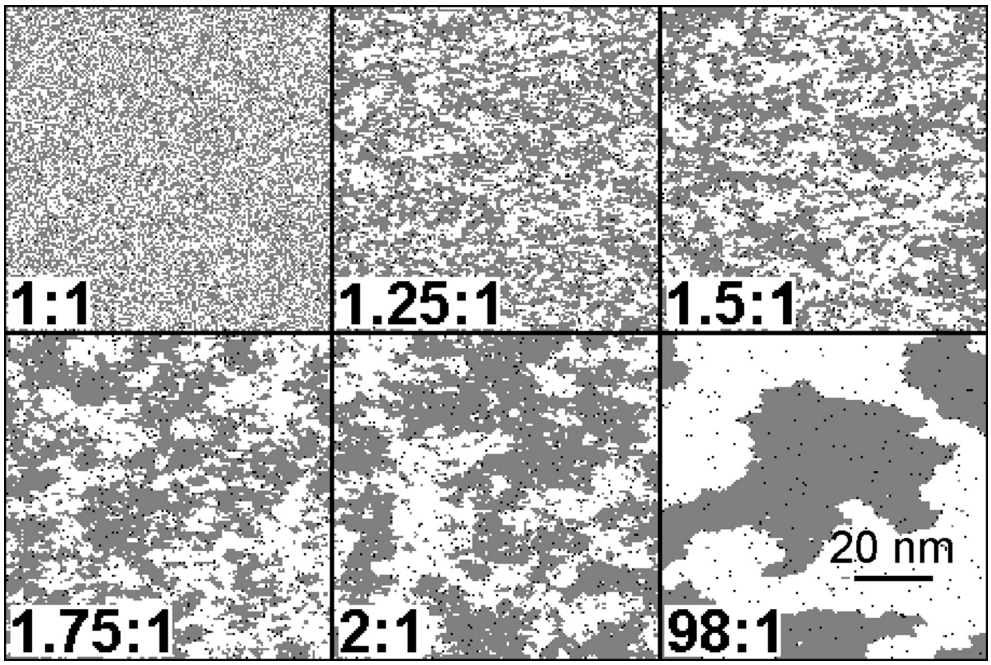

Fig. 4. Simulation patterns for different $p_{\text{same}} : p_{\text{other}}$ ratios (specified in the pictures), $p_{\text{same}} + p_{\text{other}} = 0.99$, $p_f = 0.95$. The 'h-type' binding sites are shown with white dots; the 'l-type' sites are shown with grey dots; the 'empty' sites are black. Fragments of 150×150 points from a 300×300 points simulation are shown for the 5000$^{\text{th}}$ generation.

Let us describe quantitatively such dependence of the largest domains size on the extent of preferential dopant binding. First, we need to determine which domains are the largest. Using the principle of determining the weighted median, we can define the largest domains as those with the largest sizes, which make up half of all the domains area in a given simulated pattern. Namely, if s_i, $i = 1...L$ are the domain sizes (*h*- or *l*-type) ordered by increasing, then the largest domains are those with $i > l$, where l is such that $\sum_{i=l}^{L} s_i \geq \frac{S_{h,l}}{2}$ and $\sum_{i=l+1}^{L} s_i < \frac{S_{h,l}}{2}$

($S_{h,l}$ is a general number of cells of a given type).

As it was shown by the simulation, when $p_{\text{same}} : p_{\text{other}} = 2:1$ or higher, half or more cells (typically about $3/4$) of each type comprise a single domain in a 300 × 300 simulated lattice. So, in this case, the group of the largest domains is represented by a single domain. Much higher number of the largest domains were obtained for $p_{\text{same}} : p_{\text{other}} \leq 1.5$ which corresponds to $p_{\text{same}} / p_0 \leq 1.2$. The latter parameter is more suitable to be set evenly spaced because under constant $p_{\text{same}} + p_{\text{other}}$, the value of p_0 is also constant.

The mean value of the largest domain sizes, $\langle s \rangle$, was used as a characteristic parameter for quantitative description of simulation patterns. The values of $\langle s \rangle$ for various p_{same} / p_0 are shown in Fig. 5. These values were obtained for every 500$^{\text{th}}$ generation up to 5000 and then their mean values and the standard deviations were calculated. The interval $p_{\text{same}} / p_0 = 1...1.2$ was evenly spaced; additionally, the values $\langle s \rangle$ corresponding to $p_{\text{same}} : p_{\text{other}} = 1.75:1$ and $p_{\text{same}} : p_{\text{other}} = 2:1$ are shown. Logarithmic scale for $\langle s \rangle$ is used because the range of $\langle s \rangle$ values is extremely large.

It should be noted that the value $\langle s \rangle$ for $p_{\text{same}} : p_{\text{other}} = 2:1$ actually corresponds to one large domain ($\sim 3/4$ of the total number of cells of the corresponding type). This phenomenon seems to be only caused by the size of the simulated lattice. Thus, a number of such domains will growth with increasing the lattice dimensions. However, for very large $p_{\text{same}} : p_{\text{other}}$ the domain growth seem to be defined by the lattice dimensions rather than binding probabilities at arbitrary large dimensions (an example in the case of $p_{\text{same}} : p_{\text{other}} = 98:1$ shown in Fig. 4). So, the above introduced definition of the largest domains seems poorly applicable in those cases. The values $\langle s \rangle$ corresponding to $p_{\text{same}} : p_{\text{other}} = 1.75:1$ and $p_{\text{same}} : p_{\text{other}} = 2:1$ are the mean values over 9 generations (1000...5000 instead of 500…5000), because for

such large $p_{\text{same}} : p_{\text{other}}$ the system later comes to dynamic equilibrium.

Thus, one can see that $\langle s \rangle$ growth rapidly, by *ca.* 3 orders of magnitude, with $p_{\text{same}} : p_{\text{other}}$ changes from 1 : 1 to 2 : 1. This finding affirms preferential binding as a governing mechanism of lipid domains formation in the systems explored.

It is also should be taken into account that the domains of size below ~ 100 lipid cells are less than the characteristic size of the cooperative lipid unit [41]. Therefore, domains of smaller size would hardly impact the physical properties of real lipid membranes. As we can see from Fig. 5, for p_{same} / p_0 which correspond to $\langle s \rangle > 100$ the dependence of $\langle s \rangle$ on p_{same} / p_0 shown in Fig. 5 is very close to linear (in logarithmic scale).

5. An analytical result: obtaining of bimodal adsorption isotherms irrespective of surrounding

In this section, we will show a possibility of analytical obtaining of adsorption isotherms for the case of two dopant binding modes with the binding probabilities are irrespective of surroundings. We will obtain the adsorption isotherms as the dependences of total number of cells of each type on and p_f at given p_h, p_l (we will use p_h as h-type binding probability irrespective on surroundings and p_l as the corresponding l-type binding probability).

Our general reasoning will be similar to those for obtaining canonical Langmuir adsorption isotherm, but for two binding modes instead of one. Note that Freindlich adsorption isotherms [42], rather than Langmuir ones, were established experimentally for lipid membranes in a number of experiments [1,43,44]. Freundlich isotherm is generally related to the existence of different binding sites with different energies. However, in the present work, a single type of binding sites (with two binding modes) is suggested, so the Langmuir isotherm appears.

Let S_h, S_l are the numbers of cells filled by h-type and l-type, correspondingly, and S is a common number of cells in the simulated membrane. We will determine adsorption probabilities using binding energies (see Sec. 2.3). The average number of dopant molecules adsorbing by h-type during a simulation step is $p_f p_h \dfrac{S - S_h - S_l}{S}$; the average number of desorbed dopant molecules which were h-type bonded is $\left(1 - \tilde{p}_h\right)\dfrac{S_h}{S}$. The expressions for l-type adsorption/desorption are similar. Then in the equilibrium

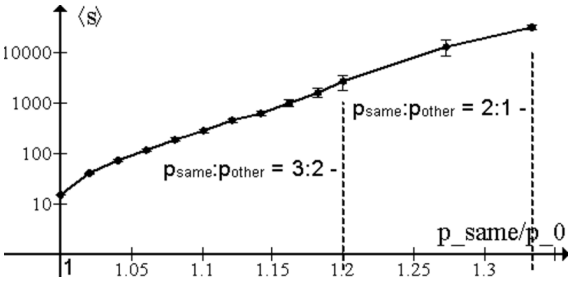

Fig. 5. The average size of the largest lipid domains as a function of p_{same} / p_0. The mean values and the standard deviations over 10 generation are shown.

$$\begin{cases} p_f p_h \left(S - S_h - S_l\right) = \left(1 - \tilde{p}_h\right) S_h \\ p_f p_l \left(S - S_h - S_l\right) = \left(1 - \tilde{p}_l\right) S_l \end{cases}.$$

So, $\dfrac{S_h}{S_l} = \dfrac{p_h\left(1 - \tilde{p}_l\right)}{p_l\left(1 - \tilde{p}_h\right)}$, we denote this ratio as κ. Then substituting $S_h = \kappa S_l$ into the second equation of the above system, we obtain

$$S_l = \frac{p_f}{\dfrac{1 - \tilde{p}_l}{p_l} + \left(1 + \kappa\right) p_f} S. \qquad (2)$$

and then

$$S_h = \frac{p_f}{\dfrac{1 - \tilde{p}_h}{p_h} + \left(1 + \dfrac{1}{\kappa}\right) p_f} S. \qquad (3)$$

According to the rules described in Sec. 2, if $p_h < p_l$, $\tilde{p}_h = 2p_h$, $\tilde{p}_l = p_l + p_h$, otherwise $\tilde{p}_l = 2p_l$, $\tilde{p}_h = p_h + p_l$.

Symmetrical case. This is the case when $p_h = p_l$ (and also $\tilde{p}_h = \tilde{p}_l$); we will further denote this value as p. For this case $\tilde{p} = 2p$. Then $\kappa = 1$ and

$$S_{h,l} = \frac{p_f}{\dfrac{1 - 2p}{p} + 2p_f} S. \qquad (4)$$

If $p_f \to 1$, $S_{h,l} / S \to p$, i.e. the membrane portions with the dopants adsorbed by l-type and h-type are equal to the binding probability. Actually, expression (4) represents the Langmuir adsorption isotherm since the total area of bonded cells is $S_h + S_l$. Generally, the result seems quite reasonable under the physical assumptions made.

Comparison the analytical and simulation results. Let us begin from the symmetrical case

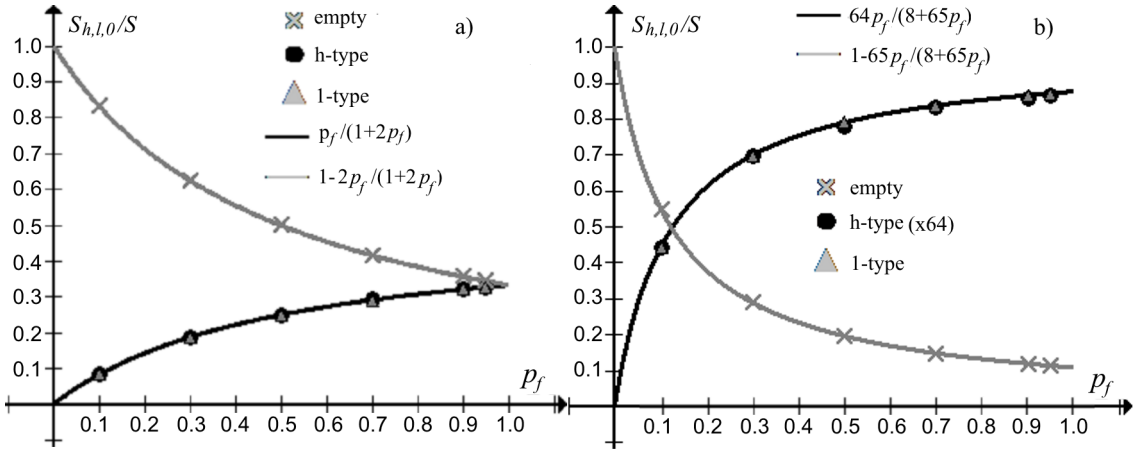

Fig. 6. Dependences of fractions S_h / S, S_l / S, S_0 / S on p_f. S_h, S_l, S_0 are the numbers of the cells with h-type and l-type dopant binding or without dopant. S is the total number of cells in the simulated membrane. A symmetrical case, Eq. 5 (a), and an asymmetrical case, Eq. 6 (b), are represented. The symbols show the simulation results; the lines are the analytical dependences. For the sake of clarity, the dependence for h-type in the asymmetrical case is re-scaled ($S_h \times 64$).

,4) and, for simplicity, assume $p = 1/3$. Then $\frac{1-2p}{p} = 1$ and

$$S_{h,l} = \frac{p_f}{1+2p_f} S . \qquad (5)$$

The corresponding simulation results are illustrated in Fig. 6, a ($p_h = p_l = 0.333$ was taken for technical reasons). The fractions of 'h-type', 'l-type' and 'empty' cells (S_h / S, S_l / S and $S_0 / S = \left(S - S_h - S_l\right) / S$, correspondingly) are shown as functions of p_f. Different symbols (circles, triangles and crosses) show the simulated values. The lines correspond to the above obtained dependence (5), which is similar for the both binding modes $S_0\left(p_f\right) = S - \left(S_h\left(p_f\right) + S_h\left(p_f\right)\right)$ normalized by S. As one can see, the simulation result coincides with the analytical one.

It is also worth comparing the simulation and analytical results obtained for an asymmetrical case, i.e. when $p_h \neq p_l$. Let $p_h = 0{,}1$, $p_l = 0{,}8$. Then we can obtain from (2), (3)

$$S_l = 64\frac{p_f}{8+65p_f} S, \quad S_h = \frac{p_f}{8+65p_f} S \qquad (6)$$

The corresponding values are shown in Fig. 6, b. As one can see, in this case, the simulation and analytical results also coincide.

Thus, the adsorption isotherms obtained in this section are completely affirmed by the corresponding simulation results; this mutually approves both the analytical discourse and the simulation procedure.

6. An assessment of some physical values corresponding to the simulation parameters used

In all the above simulations, the parameters p_f, p_{ij} were specially chosen in order to demonstrate peculiarities of lipid domains formation in various cases. Let us estimate several actual physical parameters of the system which correspond to the above used simulation parameters.

Binding energies E_i, $i = h,l$ are related to the probabilities $\tilde{p}_i$ as $\tilde{p}_i = 1 - \exp\left(-\frac{E_i}{kT}\right)$ (see Sec. 2.3). Then

$$E_i = \left[\ln\frac{1}{1-\tilde{p}_i}\right] kT .$$

In the model developed, the maximal possible $\tilde{p}_i$ corresponds to $\tilde{p}_{\text{same}}$, i.e. to the probability of dopant binding in a homogenous NN of the same type, or to the maximal of the two $\tilde{p}_{\text{same}}$ if $\tilde{p}_{\text{same}}$ is different for different binding types. So, $\tilde{p}_i$ is equal to the maximal of $\tilde{p}_{ii}$. According to the procedure of $\tilde{p}_{ij}$ obtaining using p_{ij} (see Sec. 2.3), such $\tilde{p}_{ii}$ is equal to $p_{\text{same}} + p_{\text{other}}$ for a given binding type, and we are interested in the highest of the two. Similarly, the lowest $\tilde{p}_i$ corresponds to the minimal of the two $\tilde{p}_{\text{other}} = 2p_{\text{other}}$. In the considered cases, we used the maximal $p_{\text{same}} + p_{\text{other}}$ equal to 0.99. For the largest ratio investigated, $p_{\text{same}} : p_{\text{other}} = 0.98 : 0.01$, the minimal $2p_{\text{other}}$ is equal to 0.02. This corresponds to the maximal binding energy $E_{\max} = \left[\ln 100\right] kT \approx 4{,}6kT$. This value is high enough, so it seems naturally that in this case almost all the cells become

bonded. The corresponding minimal binding energy is equal $E_{\min} = \left[\ln\frac{1}{0,98}\right]kT \approx 0,02kT$.

Dopant concentration in the solution is related to the probability p_f. Actually, p_f is the probability of a dopant molecule to appear into a tiny volume V in the vicinity of the binding site where adsorption can occur. Physically, this volume can contain more than one dopant molecule, but the model allows only one. It can be interpreted as that the volume of the dopant solution is divided into elements of the volume V, each of them can contain strictly one or no dopant molecule. According to the law of large numbers, the probability p_f is nearly equal to the fraction of such elements containing dopant molecules. Then physical concentration c_{p_f} of dopant molecules per a unit volume is $c = \frac{p_f}{V}$. The case $p_f = 1$ correspond to the system when each unit volume contains a dopant molecule, so it is the maximal concentration assumed by the model.

The volume V is approximately equal to the binding site area multiplied by a characteristic height. The area of a binding site is approximately equal to a half of the area of lipid molecule (which is ~ 60 Å^2, according to the literature [45,46]), i.e. ~ 30 Å^2. The characteristic height is reasonable to as a half of water spacing between actual lipid bilayers, i.e. ~ 8 Å [47]. Then $V \approx 250\,\text{Å}^3$. Expressing the molar concentration c_ν corresponding to p_f we obtain $c_\nu \approx \frac{p_f}{250\cdot\left(10^{-9}\right)^3}\cdot N_A^{-1} = 6\frac{2}{3}p_f$ M. For $p_f = 0,95$, as used in the above examples, $c \approx 6,3$ M.

Thus, the estimated physical parameters corresponding to the probability values used for the simulation seem quite believable.

7. Conclusions

A method of lipid domains simulation in a monolipid membrane has been developed. It consists in simulation of random bimodal adsorption/desorption of small dopant molecules in a hexagonal lattice of lipid molecules. The governing mechanism of lipid domains formation is supposed to be preferential dopant binding 'like the surroundings' rather than 'unlike the surroundings'. We ascertained that such mechanism provides formation of pronounced lipid domains, by orders of magnitude larger than the cooperative lipid unit. The lipid domains are considered as areas of connected site sets with dopant molecules bound in the same type. The domain sizes were calculated by means of a simple procedure similar to that used for percolation clusters.

Using the method allowed us to obtain the dependences of the average largest domains size on the extent of preferential dopant binding expressed as $p_{\text{same}} : p_{\text{other}}$ or $p_{\text{same}} : p_0$. The mean size of the largest lipid domains was numerically obtained as a function of $p_{\text{same}} : p_{\text{other}}$ and revealed to growth rapidly, namely, by 3 orders of magnitude with $p_{\text{same}} : p_{\text{other}}$ change from 1 : 1 to 2 : 1. This finding affirms preferential binding as a governing mechanism of lipid domain formation in the systems explored.

Adsorption isotherms for two dopant binding modes irrespective of surrounding were analytically obtained. They coincide well to the corresponding numerical simulation results. Some actual physical parameters corresponding to the probability values used in the simulation were estimated and the obtained values appeared quite believable.

The simulation method developed is relatively simple and intuitive, nonetheless it serves for gaining greater understanding possible governing mechanisms and features of lipid domains formation. Possible applications of the method might be related to physical, chemical, biological, biophysical and others systems which are similar by probabilistic properties. The method can be easily modified for exploring any systems with polymodal binding to a network of connected sites. Various lattice types or, in general, graphs of arbitrary structure can be considered. Besides, variations are possible in the amount of binding modes, in the rules for determining binding probabilities depending on the surroundings, in a number and configuration of coordination shells. Simultaneously, several kinds of dopants can be introduced and their concurrent binding can be explored. Additionally, various definitions of domains can be implemented as well as the rules for their size calculation. Any of the above modifications can result in spontaneous emergence of specific dynamic structures. So, the method may see increased application in the future.

References

1. O. V. Vashchenko, N. A. Kasian, L. V. Budianska, *et al.*, *J. Mol. Liq.*, **275**, 173 (2019).
2. N. A. Kasian, O. V. Vashchenko, L. V. Budianska, *et al.*, *Biochim. Biophys. Acta - Biomembr.*, **1861**, 1, 123 (2019).

3. O. V. Vashchenko, R. Ye. Brodskii, I. O. Davydova, *et al.*, *Eur. J. Pharm. Biopharm.*, **203**, 114469 (2024).
4. K. Simons, J. L. Sampaio, *Cold Spring Harb. Perspect. Biol.*, **3**, 10, a004697 (2011).
5. P. Sengupta, B. Baird, D. Holowka, *Semin. Cell Dev. Biol.*, **18**, 5, 583 (2007).
6. P. J. Quinn, *Prog. Lipid Res.*, **49**, 4, 390 (2010).
7. C. Altunayar-Unsalan, *Vib. Spectrosc.*, **133**, 103712 (2024).
8. Ž. Pandur, S. Penič, A. Iglič, *et al.*, *J. Colloid Interface Sci.*, **650**, 1193 (2023).
9. R. Y. Brodskii, O. V. Vashchenko, *Funct. Mater.*, **30**, 3, 413 (2023).
10. O. V. Vashchenko, V. P. Berest, L. V. Sviechnikova, *et al.*, *Int. J. Mol. Sci.*, **25**, 16, 8691 (2024).
11. O. Babii, S. Afonin, A. Y. Ishchenko, *et al.*, *J. Med. Chem.*, **61**, 23, 10793 (2018).
12. G. Albertini, E. Bertoli, G. Curatola, *et al.*, *Chem. Phys. Lipids*, **50**, 2, 143 (1989).
13. J. Matkó, J. Szöllősi, *Regulatory Aspects of Membrane Microdomain (Raft) Dynamics in Live Cells*. in: *Membrane Microdomain Signaling*, (ed. Mattson, M. P.) 15 (Humana Press, Totowa, NJ, 2005). doi:10.1385/1-59259-803-X:015.
14. N. Shimokawa, M. Hishida, H. Seto, *et al.*, *Chem. Phys. Lett.*, **496**, 1–3, 59 (2010).
15. G. Denisov, S. Wanaski, P. Luan, *et al.*, *Biophys. J.*, **74**, 2, 731 (1998).
16. D. G. Ackerman, G. W. Feigenson, *Essays Biochem.*, **57**, 33 (2015).
17. J. Huang, G. W. Feigenson, *Biophys. J.*, **76**, 4, 2142 (1999).
18. J. Huang, G. W. Feigenson, *Biophys. J.*, **65**, 5, 1788 (1993).
19. W. F. D. Bennett, D. P. Tieleman, *Biochim. Biophys. Acta - Biomembr.*, **1828**, 8, 1765 (2013).
20. S. J. Marrink, A. H. de Vries, D. P. Tieleman, *Biochim. Biophys. Acta - Biomembr.*, **1788**, 1, 149 (2009).
21. S. Baoukina, E. Mendez-Villuendas, D. P. Tieleman, *J. Am. Chem. Soc.*, **134**, 42, 17543 (2012).
22. H. S. Muddana, H. H. Chiang, P. J. Butler, *Biophys. J.*, **102**, 3, 489 (2012).
23. T. H. Ho, T. T. Nguyen, L. K. Huynh, *Biochim. Biophys. Acta - Biomembr.*, **1864**, 11, 184027 (2022).
24. P. S. Niemelä, M. T. Hyvönen, I. Vattulainen, *Biochim. Biophys. Acta - Biomembr.*, **1788**, 1, 122 (2009).
25. J. Ehrig, E. P. Petrov, P. Schwille, *New J. Phys.*, **13**, 4, 045019 (2011).
26. D. W. Allender, M. Schick, *Biophys. J.*, **91**, 8, 2928 (2006).
27. R. Lipowsky, R. Dimova, *J. Phys. Condens. Matter*, **15**, 1, S31 (2003).
28. R. Shlomovitz, L. Maibaum, M. Schick, *Biophys. J.*, **106**, 9, 1979 (2014).
29. Q. Shi, G. A. Voth, *Biophys. J.*, **89**, 4, 2385 (2005).
30. V. Pata, N. Dan, *Biophys. J.*, **88**, 2, 916 (2005).
31. R. Brewster, S. A. Safran, *Biophys. J.*, **98**, 6, L21 (2010).
32. X.-B. Chen, L.-S. Niu, H.-J. Shi, *Biophys. Chem.*, **135**, 1–3, 84 (2008).
33. Y. Jiang, T. Lookman, A. Saxena, *Phys. Rev. E*, **61**, 1, R57 (2000).
34. G. S. Longo, M. Schick, I. Szleifer, *Biophys. J.*, **96**, 10, 3977 (2009).
35. D. P. Brownholland, G. S. Longo, A. V. Struts, *et al.*, *Biophys. J.*, **97**, 10, 2700 (2009).
36. G. S. Longo, D. H. Thompson, I. Szleifer, *Biophys. J.*, **93**, 8, 2609 (2007).
37. P. F. F. Almeida, W. L. C. Vaz, *Chapter 6 - Lateral Diffusion in Membranes*. in: *Structure and Dynamics of Membranes*, (eds. Lipowsky, R. & Sackmann, E.) vol. 1 305 (North-Holland, 1995).
38. P. Garidel, W. Richter, G. Rapp, *et al.*, *Phys. Chem. Chem. Phys.*, **3**, 8, 1504 (2001).
39. Y. Jiang, K. M. Pryse, A. Melnykov, *et al.*, *Biophys. J.*, **112**, 11, 2367 (2017).
40. A. V. R. Murthy, F. Guyomarch, G. Paboeuf, *et al.*, *Biochim. Biophys. Acta - Biomembr.*, **1848**, 10, 2308 (2015).
41. N. Kasian, O. Vashchenko, L. Budianska, *et al.*, *J. Therm. Anal. Calorim.*, **136**, 2, 795 (2019).
42. H. M. F. Freundlich, *J. Phys. Chem. A.*, **57**, 385 (1906).
43. B. Tenchov, R. Koynova, *Effect of Solutes on the Membrane Lipid Phase Behavior*. in: *Handbook of Nonmedical Applications of Liposomes*, 237 (CRC Press, Boca Raton, 2023). doi:10.1201/9780429291449-11.
44. O. V. Vashchenko, *Individual and Joint Interactions of Components of Medicinal Products with Model Lipid Membranes*. (V.N. Karazin Kharkov National University, 2020).
45. J. F. Nagle, R. Zhang, S. Tristram-Nagle, *et al.*, *Biophys. J.*, **70**, 3, 1419 (1996).
46. N. Kučerka, M.-P. Nieh, J. Katsaras, *Biochim. Biophys. Acta - Biomembr.*, **1808**, 11, 2761 (2011).
47. N. Kučerka, J. F. Nagle, J. N. Sachs, *et al.*, *Biophys. J.*, **95**, 5, 2356 (2008).